The Wide Angle Camera of the ROSETTA Mission

Cesare Barbieri, Sonia Fornasier, Stefano Verani, , Ivano Bertini, Monica Lazzarin, Francesca Rampazzi
Department of Astronomy, University of Padova

Gabriele Cremonese, Roberto Ragazzoni
Astronomical Observatory of Padova

Francesco Marzari
Department of Physics, University of Padova

Francesco Angrilli, Gian Andrea Bianchini, Stefano Debei, Mario Dececco, Gianpaolo Guizzo, Giorgio Parzianello, Paolo Ramous, Bortolino Saggin, Mirko Zaccariotto
Department of Mechanical Engineering, University of Padova

Vania Dadeppo, Gianpiero Naletto, Giorgio Nicolosi, Giuseppe Tondello
Department of Electronics and Informatics, University of Padova

Pierfrancesco Brunello, Fabio Peron
Faculty of Architecture, University of Venezia

Abstract

This paper aims to give a brief description of the Wide Angle Camera (WAC), built by the Centro Servizi e Attività Spaziali (CISAS) of the University of Padova for the ESA ROSETTA Mission to comet 46P/Wirtanen and asteroids 4979 Otawara and 140 Siwa. The WAC is part of the OSIRIS imaging system, which comprises also a Narrow Angle Camera (NAC) built by the Laboratoire d'Astrophysique Spatiale (LAS) of Marseille. CISAS had also the responsibility to build the shutter and the front cover mechanism for the NAC. The flight model of the WAC was delivered in December 2001, and has been already integrated on ROSETTA.

Introduction

The study of minor bodies is of fundamental importance for the comprehension of our Solar System, because they are the bodies most representatives of its primordial material; ROSETTA is the cornerstone of European Space Agency (ESA) devoted to the study of the minor bodies of the Solar System. The primary target is comet 46P/Wirtanen, a short period comet of Jupiter family which will be reached by the spacecraft on 2012, at about 4 AU from the Sun. The spacecraft will orbit the nucleus till the perihelion in 2013, acquiring 9 months of unique data. Secondary scientific targets are two asteroids, 4979 Otawara and 140 Siwa, that will be encountered during the flight (see **Fig. 1**).

Some information regarding the S/C: box-type central structure, 2.8x2.1x2.0m height/width/depth, two solar panels with a collecting area of 32 m^2, 34 m tip to tip. The top of the S/C (+Z face, line of sight of the instruments) accomodates the instruments. The lander is attached to the -X side and a two-axes steerable HGA is mounted on the front (+X) face. The two solar wings extend from the side (±Y) faces, and their rotation is parallel to the Y axis. The Sun nominally shines in the XZ plane, and only up to (+79,-90) deg wrt the +X direction. This means

that both the side panels (+Y/-Y) and the back panel (-X) are shaded throughout all nominal mission phases, offering a good location for radiators and louvers. Furthermore this strategy limits the HGA's articulation range requirement to just over a emisphere, centred around the +X axis of the S/C. Th ±Y panels, on which the solar panels are mounted, never face the Sun during the mission. In addition, their nominally non-comet facing orientation minimises the radiator's exposure to degradation caused by cometary dust.

ROSETTA has a complex instrumentation devoted both to remote sensing and in situ investigation (see **Fig. 2**). The authors were involved in the design and manufacturing of the Wide Angle Camera (WAC) of the OSIRIS imaging system

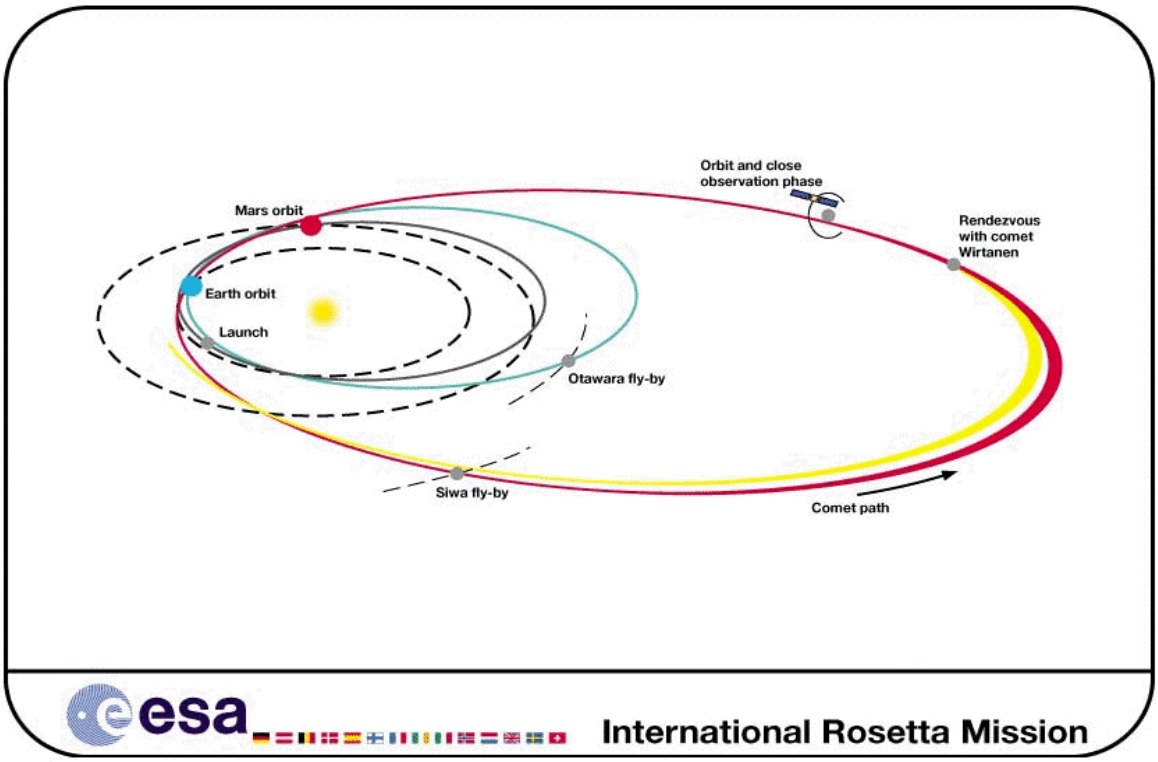

Fig. 1 – ***The ROSETTA mission***

Mission Overview

Comet 46 P/Wirtanen was discovered at Lick Observatory on 15 Jan 1948 by Carl A. Wirtanen. Two close approaches to Jupiter in 1972 (0.28 AU) and 1984 (0.46 AU) changed the orbit from an initial perihelion distance q=1.63 AU and a period P=6.71y to the present values. The comet has the following heliocentric osculating orbital elements wrt ecliptic and mean equinox of J2000.0 (from JPL Ephemeris Generator, at the date of the mission):

$e = 0.6567$, $q = 1.06$ AU, P = 5.46 y, $\omega = 82.205$, $\Omega = 356.3415$, $i = 11.723$

It belongs to the Jupiter family. The aphelion is around Jupiter's orbit. The comet was observed at all apparitions except in 1980.

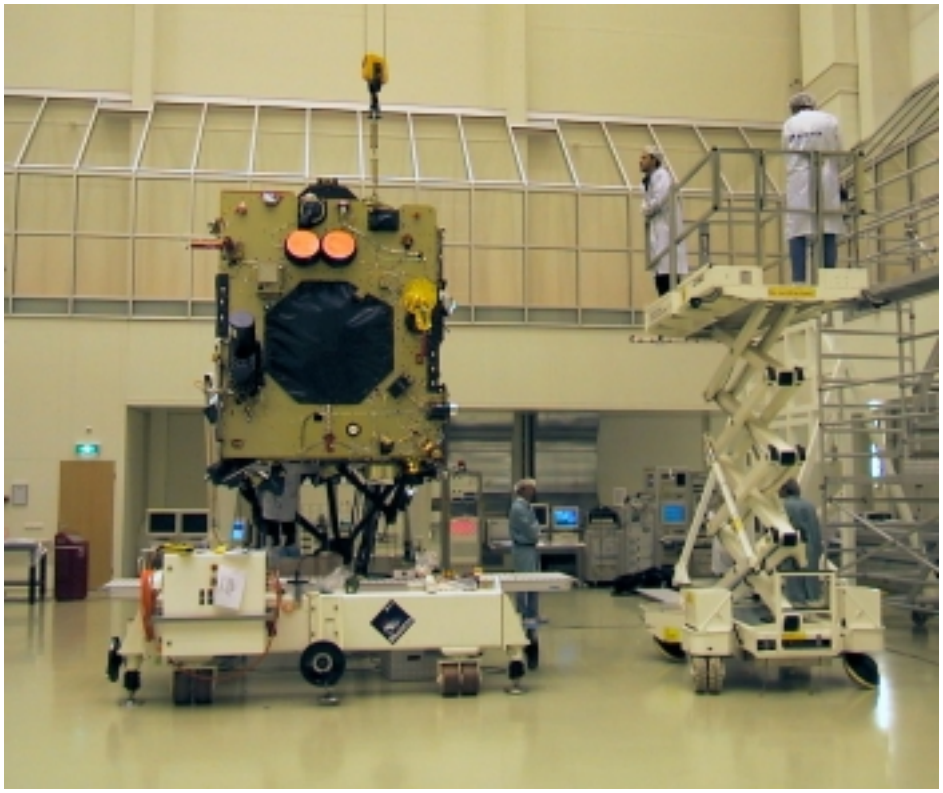

Fig. 2 – *OSIRIS mounted on ROSETTA (upper edge) , the WAC on the left, the NAC on the right, the lander that is just visible (ESTEC, Dec. 2001).*

The main steps of the ROSETTA mission are (see again **Fig. 1**):
- Launch: 20 Jan 2003, from Kourou with Ariane-5
- Commissioning phase (3 months after launch): the S/C acquires a coarse 3 axes stabilized Sun pointing attitude, and then a fine pointing attitude with the HGA Earth pointing using X band telemetry. Orbit corrections are performed. A overall checkout will be performed, including the instruments. Then the S/C wil be put to hibernation for the cruise phase to Mars.
- Earth to Mars cruise (about 950 days from launch): the S/C sleeps through the journey to Mars, a long solar conjunction prevents any operation being controlled from ground between day 440 to 690. Scientific instruments remain switched off.
- Mars gravity assist: 28 May 2005 (flyby height above surface about 200 km), distance from Sun 1.39 AU, from Earth 0.68 AU. Daily operations resume 3 months before reaching Mars. Some science operation is conducted during the swing-by (an eclipse of the Earth by Mars lasts for about 37 min).
- Mars to Earth cruise (about 90 days from Mars to Earth). The S/C is kept in 'active' cruise mode.
- First Earth gravity assist: 26 Oct 2005, perigee height 200 km. Operations are mainly devoted to tracking and orbit determination and maintenance from 3 months before until 1 month after swing-by.
- Earth to Otawara cruise (about 250 days from Earth to Otawara) : S/C put in hybernation for the cruise phase
- Otawara flyby: 10 July 2006 (around day 1270): fly-by operations last from 3 months before to 1 month after the fly-by. The scientific payload is checked out. The aim is to pass the asteroid at a distance of about 1000 km on the sunward side. The relative asteroid ephemeris will be determined with a cross track accuracy of 20 km by S/C optical navigation. The cameras and scientific payload will point in the direction of the asteroid until after the flyby. Science data will be recorded in the mass memory and transmitted to Earth after the flyby, when the Earh link with the HGA is recovered.

- Otawara to Earth cruise (about 450 days from asteroid to Earth), the S/C is in a dormant phase.
- Second Earth gravity assist: 27 Oct 2007, perigee height about 2200 km. Operations are essentially the same as for the first swing-by.
- Earth to Siwa cruise, about 250 days, S/C dormant
- Siwa flyby: 23 July 2008, around day 1980. Operations are similar to the Otawara flyby, although at a larger flyby distance.
- Asteroid to comet cruise, about 1200 days from asteroid to comet rendez-vous manoeuvre. The S/C is in hybernation. Maximum distance of S/C from Sun (aphelion): 5.1 AU at beginning 2011; maximum distance from Earth 6.2 AU
- Rendez-vous manoeuvre around day 3140. The S/C relative velocity is decreased to about 25 m/s. It will be performed before the comet is detected by the on-board cameras, using ground based determination of the comet nucleus orbit with a dedicated astrometric campaign.
- Encounter with P/Wirtanen: 27 Nov 2011 at 4.5 AU
- Near-comet drift phase (700 days): when the solar distance is below 4.2 AU the actual approach operations can be started. The selection of this final point depends on two factors: avoiding cometary debris and achieving good comet illumination conditions. The final point is the Comet Acquisition Point (CAP) where the comet will be observed by the on-board navigation cameras or by OSIRIS for the first time. During this phase, the S/C is in active cruise mode.
- Far approach Trajectory Phase (up to 90 days), starts after CAP. After detection, knowledge of the comet ephemeris will be drastically improved by the processing of on board observations. Image processing on ground will derive a coarse estimation of comet size, shape and kinematics. The approach manoeuvre sequence will reduce the relative velocity in stages, slowing to 2 m/s after 90 days. The strategy will be designed to: retain an apparent motion of the comet with respect to the star background; retain the illumination angle (Sun-comet-S/C) below 70°; avoid the danger of impact with the cometary nucleus. The Far Approach Trajectory ends at the Approach Transition Point (ATP) which is the point where a first estimate of the comet attitude, angular velocity and location of landmarks is obtained from the analysis of the navigation camera or OSIRIS images. The ATP is located on the Sun direction at about 300 comet nucleus radii from the nucleus. During this phase the S/C is in active cruise mode with the navigation camera system and some orbiter payload switched on.
- Close approach trajectory phase, starts at ATP. Line of sight landmarks are processed together with on-ground radiometric measurements in order to estimate the S/C relative position and velocity, comet absolute position and attitude, nucleus angular velocity, gravitational constant and location of landmarks. The end of this phase is the Orbit Insertion Point (OIP), where the S/C is injected into a hyperbolic arc to the comet, at a typical distance of 60 comet radii and a velocity of some cm/s.
- Transition to a Global mapping phase, starts at OIP, a hyperbolic arc is used down to a distance to the comet of about 25 radii, when a capture manoeuvre will close the orbit. The plane of motion is defined by the spin axis and by the Sun direction, and rotated slightly to avoid Solar eclipses and Earth occultations.
- Global Mapping phase: the preliminary survey of the surface of the comet. At least 80% of the surface subject to solar illumination is required to be mapped. Polar orbits at a distance between 5 and 25 radii will be used for mapping on the surface. The orbital periods will be usually greater than the spin period. Horizontal swaths will cover the nucleus surface as it is presented. The semimajor axis of the mapping orbit will be chosen as a function of comet gravity and spin rate. In case of a slowly rotating nucleus, it may be necessary to use more than one revolution in the same orbit or a second different orbit by means of plane change maneuvers. At the end of this phase some 5 areas of 500x500 m will be selected for close observations.
- Close observations (up to 30 days) of the selected points, avoiding debris, dust and gas jets. The observed areas must be under illumination and the angle between viewing direction and normal to

the local surface below 30 deg. At the end of this phase a decision will be taken at which site the Surface Science Package (SSP) will be delivered.
- Surface package delivery and relay (20 days). Delivery will be from an eccentric orbit (pericenter altitude as low as possible, e.g. 1 km), at the lowest possible velocity relative to the (rotating) surface. After delivery, the S/C will be injected into an orbit best suited to receive the data transmitted from the SSP and to relay them to the Earth.
- Extended monitoring phase (up to 240 days through perihelion), after the end of the activities related to the SSP. The objective of this phase is to monitor the nucleus (active regions), dust and gas jets, and to analyse gas, dust and plasma in the inner coma from the onset to the peak activity. Extended monitoring could be performed by successive hyperbolic flybys configuring petal-like trajectories
- Perihelion date: 10/07/2013, around day 3800, end of nominal mission.
Operations and orbit determination will be carried out by ESOC.

The WAC optical configuration

The optical configuration of the WAC was selected in a trade-off procedure among different configurations in order to satisfy the following initial scientific specifications:
- field of view (FoV) of 12°x12°, Focal Lentgh (FL) about 140mm, final F/5.6 numerical aperture
- contrast ratio of 10^{-4}, in order to detect gaseous and dusty features close to the nucleus of the comet
- collecting aperture of about 5 cm^2, allowing detection of the cometary nucleus and of the asteroids from a distance of 10^6 km in 1 second exposure time
- UV overall efficiency, and durability in the Solar System for 10 years.

The WAC finally built and about to fly has the following characteristics (**Table 1**):

Table 1 - *F/5.6 WAC Optical Characteristics*

Optical concept	all reflective, 2 mirrors 20° off-axis design, unobstructed, unvignetted Axis of off-axis: *y*
FoV	(12°.00 in *x*)∗(12°.05 deg in *y*)
Encircled Energy	80% inside pixel of 13.5 μm
FL at center of FoV	132 mm
Image scale at the center of FoV	1562.6”/mm (7.58mrad/mm)=21.1”/px (102.3μrad/px), px = 13.5 μm
Distortion of the field	Barrel type
FL in *x*	varies from 126 mm to 135.6 mm from top to bottom
FL in *y*	varies from 128 mm to 133 mm from right to left
Residual geometrical distortion	<1% using the respective image scales
Refocusing	no refocusing necessary for distance range 500 m to infinity
Nominal F/ratio	F/5.6 (linear aperture: 25 mm, photometric area $(1.25)^2$= 4.91 cm^2)
Wavelength range	230 to 750 nm
Overall reflectivity	from 65% at λ 240 nm to 72% at λ = 800 nm
Filter wheel	dual filter wheel, 8 positions each, 7+7 square filters and 1+1 square hole
CCD rows	aligned along *y* axis of optics
CCD columns	aligned along *x* axis of optics
Shutter blades	aligned along *x* axis of optics
Blades flight direction	along *y* axis

The primary mirror (M1) is an off-axis section of an *oblate convex ellipsoid*, decentered with respect to the optical axis of 43 mm and of squared shape (53×53 mm^2); the second one (M2) has an *oblate concave ellipsoidal shape*, 5 mm decentered with respect to the optical axis of the camera. The equation of the two mirrors is that of conic sections:

$$z = cr^2 /(1+\sqrt{1-(1+k)(cr)^2})$$

where the parameters are

M1: 18 mm < r < 68 mm, k = 5.7079, $R = 1/c$ = 406.6157 mm;
M2: 0 < r < 32 mm, k = 0.1656, R = 400 mm.

M1 collects the light from the object at an angle of 20° with respect to the camera axis and sends it to M2, which focuses the light on the focal plane assembly placed 51 mm behind M1. The system stop is at the level of M2 and it is decentered by 5 mm with respect to the optical axis.

Fig. 3 shows a sketch of the optical design; the detailed optical calculations have been performed inserting in the optical design a wedge-shaped filter, at λ = 610 nm, and a fused silica (Suprasil) 4 mm thick plane (for CCD shielding reason). The off-axis design produces two slightly different image scales: the scale in x varies from 21.8''/px to 20.4''/px. Therefore the field width in x decreases from 12.4° to 11.6°, while it is constant, 12.05°, in y. The nominal photometric aperture is circular, with a radius of 1.25 cm; however, the distortion just described causes the aperture to be slightly elliptical and position dependent. The corresponding photometric variations will be removed both by calculations and by calibrations.

Regarding the imaging properties for an object at close distance, the performance is kept essentially unchanged from infinity down to almost 500 m. The average spatial scale and total imaged linear field at various distances of the S/C from the object are shown in **Table 2**.
With the respect of the Optical Reference Frame (see **Fig. 3**), the CCD rows are aligned in y, while the CCD columns in x (perpendicular to the incidence plane yz). Accordingly the shutter slit is aligned in x, the blade travel direction is in y.

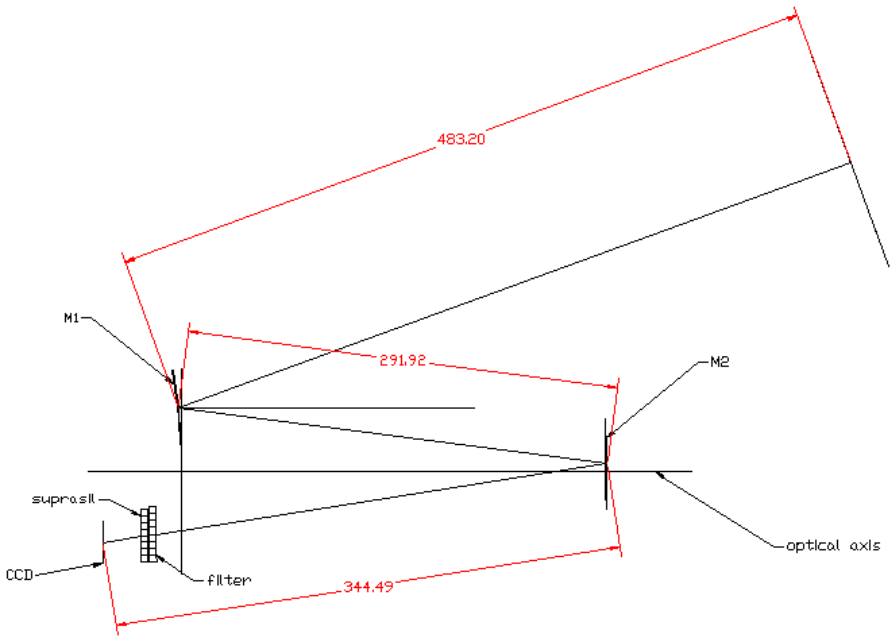

Fig. 3 – *Optical design and dimensions of the optical train*

Table 2 - *Percentage of Energy inside the pixel*

Field	X-angle	Y-angle	Infinity	2 km	1 km	0.5 km
1	0.00	20.00	0.74	0.75	0.76	0.76
2	0.00	14.15	0.76.	0.75	0.73	0.69
3	0.00	26.20	0.80	0.79	0.78	0.74
4	5.80	14.15	0.77	0.77	0.76	0.72
5	6.00	20.00	0.78	0.79	0.80	0.78
6	6.20	26.20	0.74	0.75	0.76	0.72
7	-5.80	14.15	0.78	0.78	0.76	0.72
8	-6.00	20.00	0.78	0.79	0.80	0.78
9	-6.20	26.20	0.75	0.75	0.75	0.72

Fig. 4 shows the energy distribution at the various angles over the FoV.

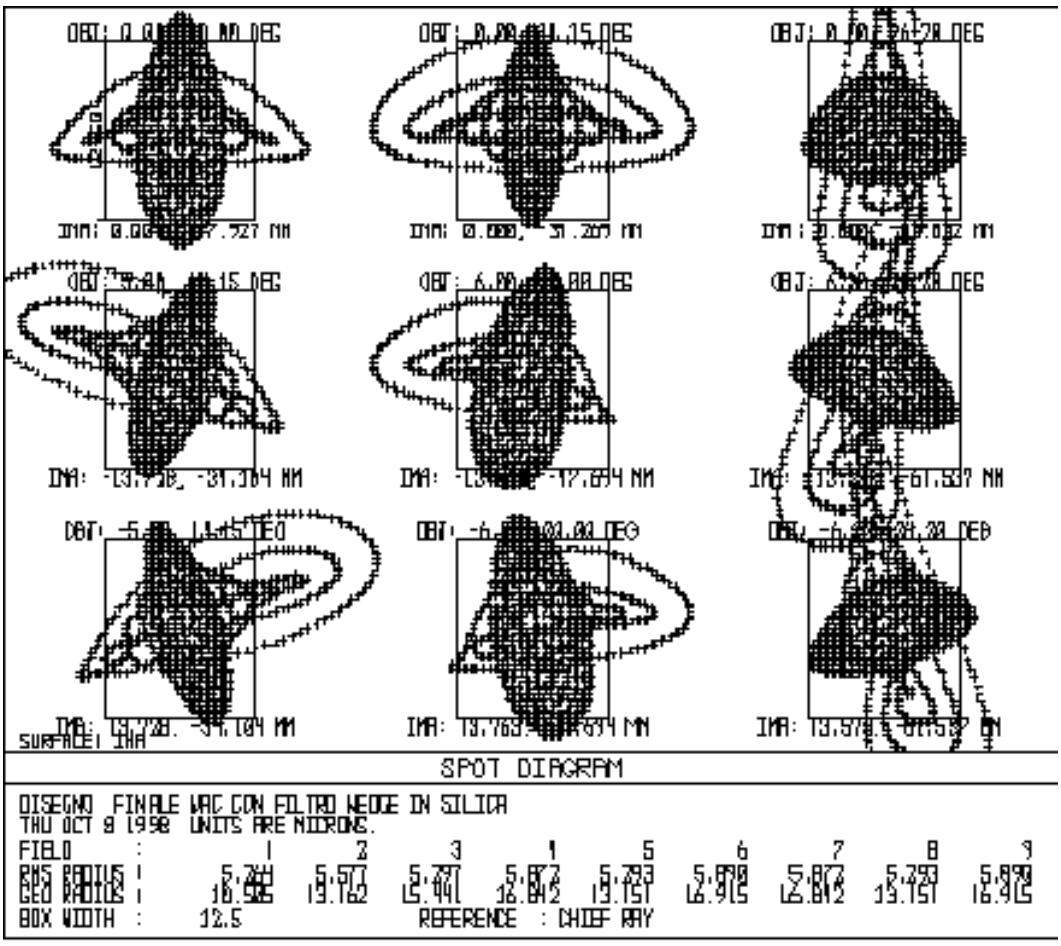

Fig. 4 – *Ray tracing over the FoV. The size of the square is 13.5 μm.*

The average spatial scale and total imaged linear field at various distances of the S/C from the object are shown in **Table 3**.

Table 3 - *Mean scale and field as function of distance*

Distance (km)	Resolution	Field (km)
0.6	0.06 m/px	0.13
1.0	0.10	0.21
3.0	0.33	0.65
6.0	0.60	1.3
10	1.0	2.1
30	3.3	6.5
100	10.0	21
1000	100	210
10^4	1 km/px	$2x10^3$
10^5	10 km/px	$2x10^4$
10^6	100 km/px	$2x10^4$
$1.5x10^8$ (1 AU)	$1.5x10^4$ km/px	$3x10^7$ (0.2 UA)

Mirrors have been produced and polished by Officine Galileo, with performances reaching specifications. For better surface finish the selected material is Schott BK-7. The mirrors have been aluminized and protected with MgF_2. **Fig. 5** shows one pair of M1 and M2.

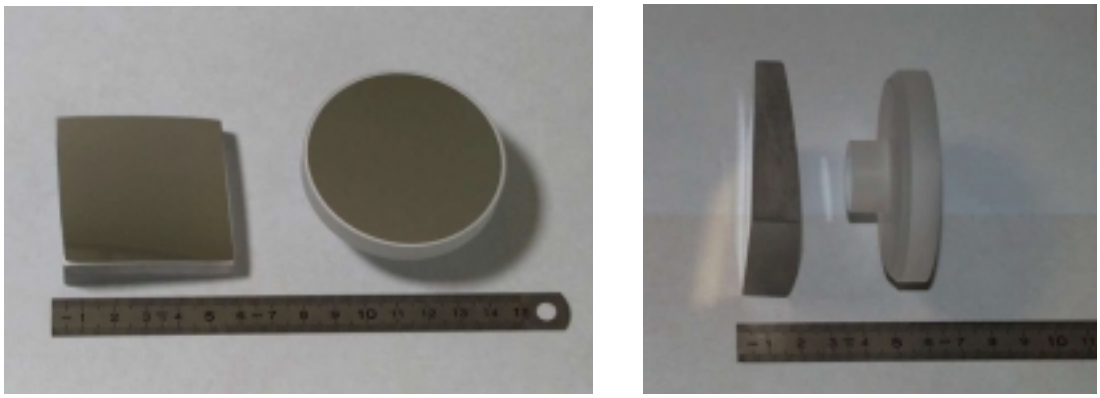

Fig. 5 – *M1(left) and M2 (right), as seen from the front and from the side. Notice the convex shape and strongly aspheric shape of M1; M2 is also slightly aspheric, and protrudes on the backside for easier mechanical mounting.*

Table 4 gives the expected reflectivity of 1 and 2 mirrors (after 8 years in orbit).

Table 4 – Expected Reflectivity of the WAC after 8 years in orbit

λ (nm)	R	R^2	λ(nm)	R	R^2
240	0.77	0.60	500	0.80	0.64
280	0.77	0.60	550	0.80	0.64
300	0.78	0.61	600	0.80	0.64
350	0.79	0.62	650	0.80	0.64
380	0.89	0.63	700	0.79	0.62
400	0.80	0.64	800	0.77	0.60
450	0.80	0.64	1000	0.82	0.67

The optics of the WAC have been mounted and tested inside a dedicated clean room, shown in Errore. L'origine riferimento non è stata trovata.. The clean room has a useful surface of 35 m^2, with standard M3.5/M4.5 (class 10000/100). It is provided also with a laminar flux bench (class 100) used for instance to glue the mirrors to their supports, and an optical bench 1.25 m × 2.5 m in class 100. Available equipment comprises the following elements:

- CCD camera (1300 × 1030 pixel) for general purpose alignment activity, with frame grabber and beam analyzer; a 10× magnifier can be coupled to it
- Zygo interferometer
- Continuum VIS/UV source with fiber optics output

The WAC filters

A set of 14 filters for the WAC (and 12 for the NAC) has been carefully selected for maximum scientific return; their list is provided in **Table 5**. The filters were produced by Spectrogon (Sweden), under the supervision of the Lund Observatory.

Table 5 - *List of WAC filters*

λ	Δλ (FWHM)	T %	Objective	Wheel 1 P	Wheel 2 P	Code
245	15	>35	Continuum; backup for surface reflectance	2	1	21
257.5	4	>25	CS gas emission	3	1	31
295	10	>35	Continuum for OH	4	1	41
308.5	4	>25	Detection of OH emission from vicinity of nucleus	8	1	81
325	10	>35	Continuum for OH; backup for surface reflectance	1	5	15
335.5	4	>25	NH gas emission	1	7	17
375	10	>50	Continuum for CN, backup for surface reflectance	5	1	51
387.5	4	>25	CN gas emission	6	1	61
535	60	>70	V dust continuum	1	8	18
571.5	10	>25	NH2 gas emission	7	1	71
589.1	4	>25	Na gas emission	1	2	12
610	10	>50	Continuum for OH; backup surface reflectance	1	3	13
630	4	>25	O (1D) gas emission for dissociation of H2O	1	4	14
640	160	>90	Broad band R	1	6	16
Empty						
Empty						

In the case of the WAC, one principal aim is to study the intensity of gas emissions and dust-scattered sunlight as functions of position and viewing angle in the vicinity of the nucleus. This is accomplished by centering narrow passbands on a set of emissions expected to be both strong and diagnostic of physical processes in the comet, and to separate out relatively emission-free but broader passbands to study the dust as uncontaminated by gas as possible. Most of the latter are chosen to provide continuum measurements close to the gas emissions in order to remove any dust contributions within the emission passbands. The central wavelengths span from 245 to 640 nm. For the gas emissions the bandwidth is 4 nm, the minimum allowed by the F/5.6 optical design. One continuum filter has a very wide passband in the R spectral domain and is aimed to help detecting the cometary nucleus and asteroids at large range. This is the filter we concentrate in the present discussion. With nearly 11 years flight in interplanetary space before the start of cometary observations, one needs to ensure that the performance of the filters is not seriously downgraded by cosmic ray damage. Many of the substrates are made of Suprasil, which is known to be radiation hard, but in other cases Schott coloured glasses to help ensuring a proper out-of-band blocking were used. Since too little was known about the radiation hardness of such glasses, and unacceptable damage levels could not be excluded, laboratory experiments with the Uppsala tandem Van de

Graaff accelerator were performed. A 2 MeV proton beam was shot onto OG590, KG3, and Suprasil glasses to simulate the solar wind proton exposure during the Rosetta cruise and measured the resulting change in spectral transmission. The general conclusion is that the expected damage levels are indeed acceptable.

The filters are placed relatively close to the detector in the optical path. This minimizes the required size of the filters but, because of the large CCDs used by OSIRIS, the physical sizes of the filters are still fairly large. The required clear aperture is 37.5 mm x 37.5 mm. The filters are square with rounded-off corners. The physical size is 40.0 mm x 40.0 mm. The filters are wedged to reduce ghosts and are optimized for operation at +10C. The filters for the WAC are tilted by 8°.7 to the incoming beam (the filters for the NAC are tilted by 4°.5) to the incoming beam.

The NAC and the WAC suffer from a complex combination of ghost images because of the presence of three transmission elements in front of the CCD. Two types of ghosts may be distinguished. The "narcissic ghosts" are caused by light reflected by the CCD surface and back reflected from transmission elements. "Filter ghosts" are caused by two successive transmissions from transmission elements. The ghost images are out-of-focus replica of the scientific image and the amount of defocus is different for each ghost image according to the extra optical path traveled. For a point source, the diameter of the ghost image increases with increasing optical path and so the ghost intensity decreases. For extended objects however, such as the comet nucleus, the integrated ghost intensity is independent of defocus distance and equals the product of the two reflections encountered. In order to take advantage of cases where one ghost type is weaker than the other, the two types are physically separated. This is achieved by introducing a tilt of the filter wheels with respect to the optical axis, sending filter ghosts to one side of the scientific beam and narcissic ghosts to the other side. The slight dispersion effect introduced by this tilt is compensated by the wedge of the filters.

Regarding the WAC, the beam incidence is not normal. The non-wedged surface of the filter is parallel to the CCD plane which is orthogonal to the camera optical axis. The angle between the optical axis and the chief ray of the light beam is 8.92°. The thickest filter side is toward the filter wheel rotation axis. Ghost minimization with suitable AR coatings is even more stringent than for the NAC because of the initial contrast requirement. An analysis of the ghost images has shown that the Secondary Narcissus ghost (SNgh) is the most intense one. This ghost is produced by the back reflection of the beam both from the CCD surface and the filter surface farthest from the CCD. The ratio of total SNgh over total image intensity, (where total means that is integrated all over the wavelength range), depends on the filter and is 0.16 for the worst case (NH filter) and 10^{-3} for the best case (Green and R filters).

During tests of the Flight Model, the WAC UV filters showed the presence of small pinholes, that went undetected during the acceptance tests; after considerable discussion, and given the pressure with the delivery of the flight model, no correcting action was taken; therefore the WAC UV images will require careful flat fielding in flight.

The Filter Wheel mechanism

The filters are mounted on a dual Filter Wheel Mechanism (FWM), shown in Fig. 6 and produced by INTA (Spain), that places the optical filters in front of the CCD sensors on both WAC and NAC cameras. Each filter wheel assembly is composed of:

- a support structure
- a common shaft with two filter wheels (each one has its own position monitoring system and a magnetic locking device)
- two steeper motors with harness and a 44 pin connector
- two gears with parallel teeth (the pinion is attached to the motor, and the crown to the disk)
- a set of fourteen glass filters.

The filters are distributed over the two parallel wheels. The only qualitative difference between the WAC and NAC FWMs is in the filters combination installed on them. Each FWM has the possibility of positioning up to 14 different optical elements (7 filters and a refocusing element installed in NAC and 7 filters and a hole in WAC). Each filter wheel is commanded by a step motors, capable to place in position the worst case filter (half wheel turn) in less than 1.5 s. All filters must be positioned in front of the CCD within ±135 μm (10 CCD pixels), and must guarantee ±30 μm of repeatability (2 pixels). This is achieved by means of a magnetic locking device acting over each wheel. Each of the seven filters is verified by a position monitoring system using a four bits code formed by radially arranged SmCo magnets which are detected by a parallel array of four Reed switches. All magnets are placed on top of plates made of a high permeability and soft ferromagnetic materials (i.e. mumetall). The function of these plates is to isolate the magnetic field coupling between the wheels.

Given the tight requirements of mass, power, commanding time and thermal operational limits, a titanium alloy for the FWM shaft and an aluminium alloy for the rim wheel and the assembly support were employed. The filter wheel support has three mechanical interface points of fixation with adjusting shims, to allow its correct alignment on the cameras. The rim wheel also supports the crown gear made in Vespel. The reduction gear pinion is made of stainless steel, and fixed to the motor shaft by means of a screw and EC2216 glue. This material combination has been previously used in other space mechanisms applications. The gap between pinion and crown (jamming) was adjusted around 50μm, which is equivalent to 0.07^{o} backslash in the wheel. The gear reduction of 9:1 fits very well with the motor wheel characteristics, avoiding the stop of the same pinion tooth in each filter position, and increasing the pinion life. Total mass for the FWM is (1450 ± 3) g, and the total moment of inertia is: $I_{xx} = 3.41 \cdot 10^{-3}$ kg·m^2, $I_{yy} = 2.83 \cdot 10^{-3}$ kg·m^2 and $I_{zz} = 5.41 \cdot 10^{-3}$ kg·m^2. The step motors are the SAGEM 11PP92 model, modified to supply a higher holding torque of 300 cNcm with a power of 10.5 W. Those motors have redundant coils and work without any step loss by means of a ramp control during the commanding.

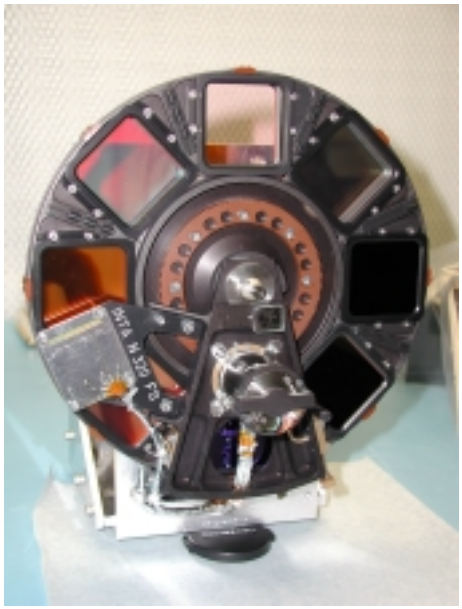

Fig. 6 – *The Filter Wheel Mechanism*

The optical bench

The lightweight and high stiffness structure concept is based on a closed box made of Aluminum alloy engraved by electro-erosion (see **Fig.7** and **Fig. 8**). The optical bench ribs are optimized to fulfil the optical performances at the higher frequencies, preventing the noise that may be introduced by the dynamic environment of the spacecraft and minimizing the amplification at the interfaces with mechanisms. The vibration tests made both at unit and a system level showed a first eigen frequency of about 170 Hz, within 5% of that predicted on the basis of the mathematical model. The camera is attached to the spacecraft by means of 3 kinematic mounting feet in Titanium alloy.

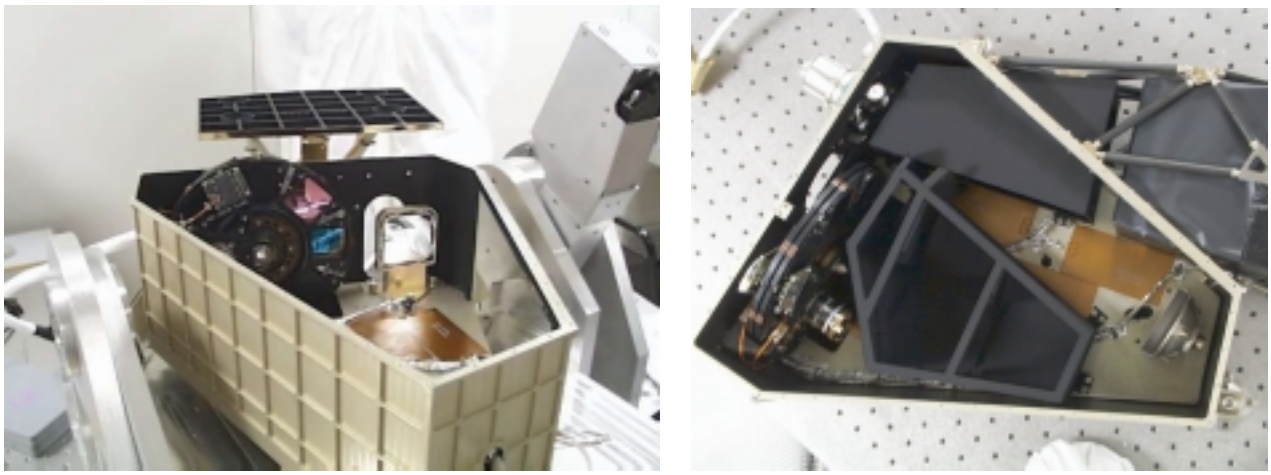

Fig. 7 – *The camera as seem from above in two different stages of mounting. a) the left panel: before insertion of the baffles, M1, the dual filter wheel and the CCD radiator are seen. b) right panel, upper right: the external baffle with its attaching frame. The primary mirror M1 is on the upper left, inside the second section of the baffle. On the right, M2 is seen, then the inner baffle, and the dual filter wheel. The Focal Plane Assembly will be mounted on the external wall to the left. On the upper left, the shutter mechanism, with one encoder encasing protruding outside. On the lower right, one of the 3 mounting feet is visible. On the floor, the heaters for thermal control.*

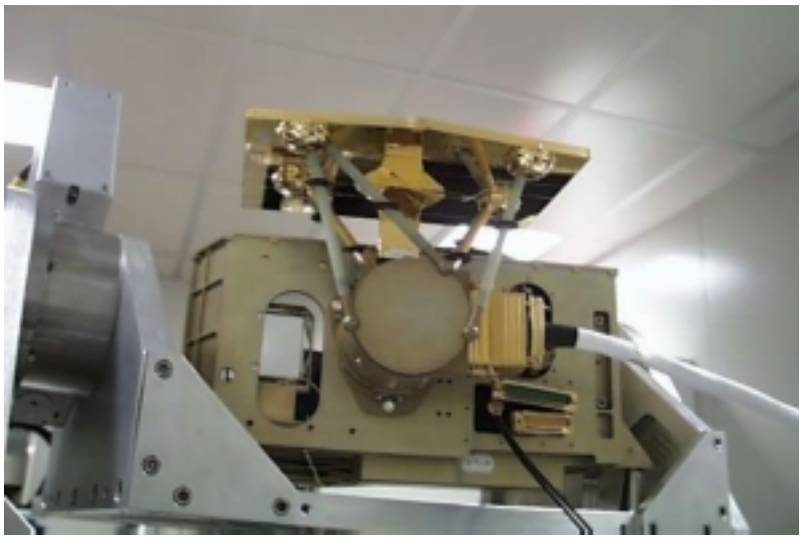

Fig. 8 – *The Focal Plane Assembly mounted on the rear of the optical bench. Notice the upper heath radiator for passive cooling of the CCD.*

The telescope is covered by a thermal blanket, while the inner parts have been black-painted with electrical conductive paint.

To minimize distortion the supports of M1 and M2 are made of the same material of the optical bench, so that the elastic mounting of the BK7 mirrors are optimized in relation to the optical requirement (see **Fig. 9**).

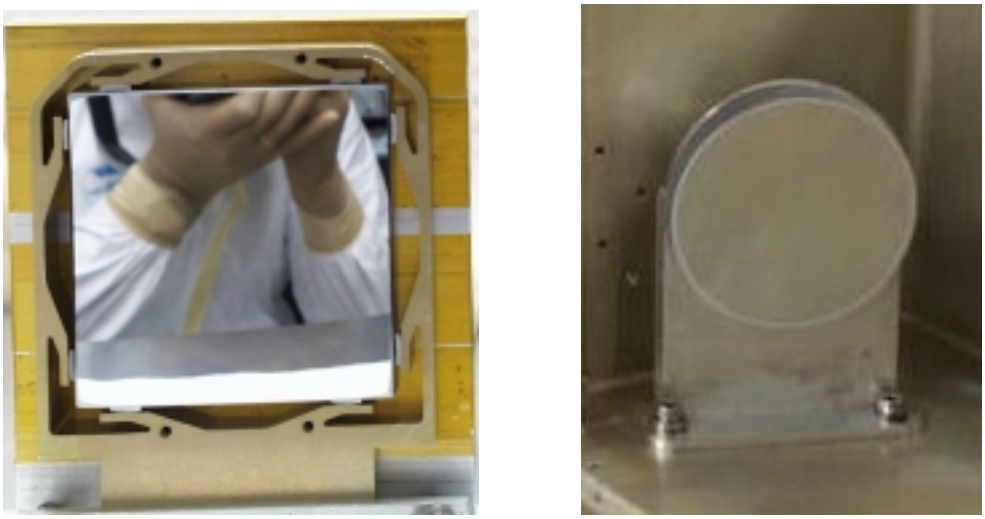

Fig. 9– On the left, the mounting of M1, on the right the mounting of M2.

The WAC thermal control system has to cope with the stringent requirement about the temperature range of ± 5°C allowed for the optical bench during operation. The challenging requirement derives from the allowed tolerances in the positions of the telescope optical elements inherent to the adopted optical scheme. The total electrical power dissipated into the camera is less than 2 W, even in the high power mode, while the heat leak from the FPA is of the order of 1 W.

With only 1 W to dissipate a during the high power mode the camera should ideally be thermally insulated as much as possible from the environment. To do so, the whole external surface has been covered with a MLI insulator and the mounting on the S/C by insulating feet made in Titanium alloy (see again **Fig 7**). The stronger disturbances to the WAC thermal control come from the large optical aperture, a surface of about 300 cm^2 at baffle input that is facing environments ranging from the cold space to the comet plus a Sun incidence angle of 11°, at a Sun distance of 1 AU. The external baffle was the most critical element in the thermal design, therefore a trade-off analysis had to be performed considering various combination of materials, thermo-optical coatings and mountings. A Glass Reinforced Epoxy structure with total absorber coating, conductively insulated from the camera, proved to be the best solution. To extend the operational capability to the condition of Sun incidence angle of 45°, a radiator has been added in the upper part of the baffle to reduce the heat flux on the camera. The thermal control system allows to operate the camera from the detection phase, when there is no external heat flux and the expected spacecraft temperature is -30 °C, to the comet perihelion, with a Sun incidence angle of 45° and an expected spacecraft temperature +50 °C. This is achieved using 12 W for the operational heaters used to compensate for the heat loss in cold configurations. Operation of the camera at sun incidence angles smaller than 45° is foreseen only intermittently, with phases of cooling with closed entrance door followed by observations with the door open, until the allowed upper temperature limit is exceeded.

The other important requirement for the camera thermal control system is providing a temperature higher than –40 °C during the non operative phase; this goal is achieved using an electrical heater dissipating 5 W.

The baffling system

The very peculiar optical system, based on two aspherical mirrors in an-off axis configuration, and the primary scientific aim to study very faint gas and dust cometary features in the vicinity of the nucleus at all heliocentric distances from 3.2 AU (start of the nominal mission) to the perihelion, imposed the design and construction of an innovative baffling system, in order to reach the stray-light suppression requirements both for source inside and outside the field of view of the camera. In particular a contrast ratio of 10^{-4} inside the field of view is needed in order to detect gaseous and dusty features close to the nucleus of the comet. The WAC baffle system has therefore to perform two different and quite tightening functions. First of all the attenuation of the light coming from any source outside the FOV; in this regard stray-light attenuation ratio baseline is $4x10^{-9}$ at 45° off-axis. Additionally because of the peculiar solution adopted for the optics, only part of the radiation reaching the instrument within the FOV is focused onto the detector; therefore the rest, scattered inside the instrument, become stray-light and, consequently, must be suppressed. For the light inside the field of view attenuation ratio must be less than 10^{-4} in order to detect the weak features (dusts and gases) associated to the coma.

The baffling system is made by two main parts: the first one with rectangular cross section is localised in front of M1 mirror and has 17 vanes; the second one is localised between M2 and the detector and has 4 deep vanes (see **Fig. 10**).

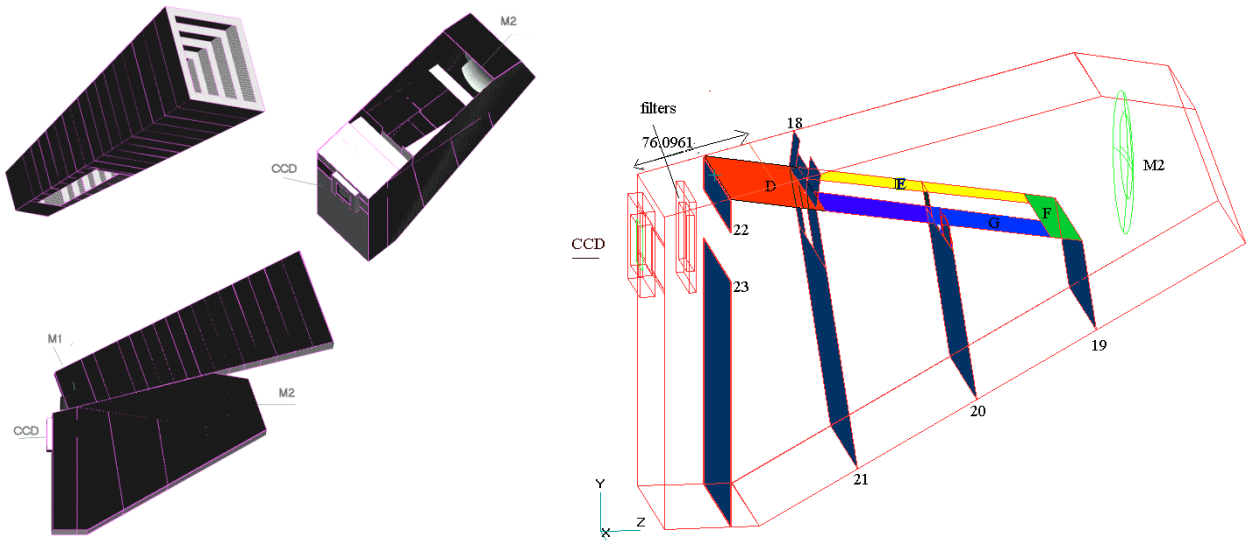

Fig. 10– *The baffle before M1 (upper left) is actually composed of two structures mounted together; the internal structure in its turn is composed by two boxes.*

The external section is made in fiber glass, and is attached to the camera structure by means of a very light frame in carbon fiber (see **Fig. 11** and **Fig. 12**), which improves the thermal decoupling between the external baffle and the optical bench, and minimizes the temperature gradients. The baffling system was completed by adding two blackened rims around M1 and M2.

During the tests in the laboratory, a very narrow cone of direct light going in the proximity of the Focal Plane Assembly area was discovered. This light leakage was closed by inserting two additional vanes in blackned Kapton just after M1 and before the shutter (see **Fig. 13**).

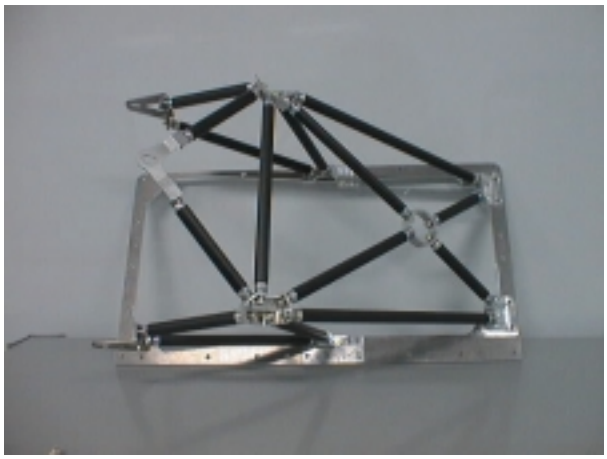

Fig. 11– *The carbon fiber frame connecting the external baffle to the camera structure.*

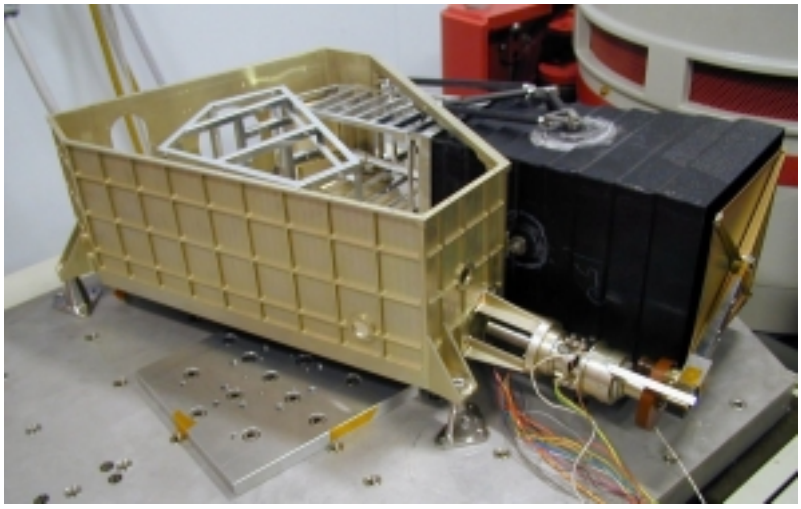

Fig. 12 – *A view of the entire baffling system, before painting and covering with blackened kapton tape. The external section is closed by the front door, whose mechanism is in front (this image refers to the QM)*

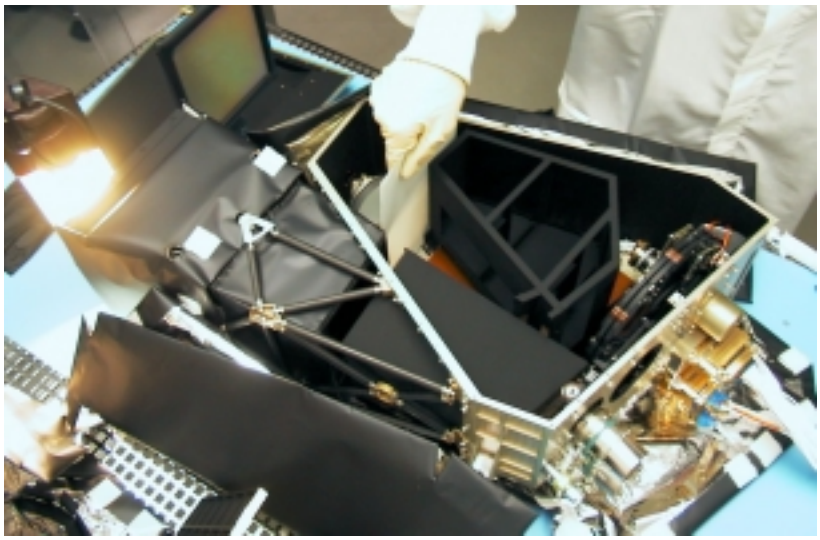

Fig. 13– *checking for stray light on the optical laboratory with a bright lamp (upper left).*

Two calibration lamps will be used in flight for internal flat fielding. The lamps, provided by LAS, have characteristics similar to those used for LASCO (Welch Allyn bulb lamp flame-formed, *T*(col) = 2410 K, life time 4000^h, current 0.35 A at 2.5 V, weight = 11.0 gm each). No UV light is emitted. Two are foreseen for uniform illumination, plus two for redundancy. The lamps have been mounted on the fifth vane of the external baffle. They illuminate the backside of the front door cover.

The shutter system

The shutter is electromechanical instead of electronic in order to guarantee the best performances in terms of S/N ratio. The shutter goal is to guarantee exposure times within the range 10ms - 100s, with a minimum repetition rate of 1s for high speed imaging mode. The normal case should be around 100ms for a repetition rate of 15s. The most challenging requirement is the uniformity of 1/500 for pixels integration time. Taking into account that the 2048 x 2048 CCD has a pixel size of 13.5 x 13.5 μm, it leads to the global size of 28 x 28 mm. At the level of the achievable S/N ratio, that is >300 per pixel, and >600 for 2x2 pixel binning. Binning in the DPU can achieve S/N ratios greater than 1000.

The shutter is made up of two blades driven by two independent four-bar-mechanism devices (**Fig. 14**) moved by two brush-less motors.

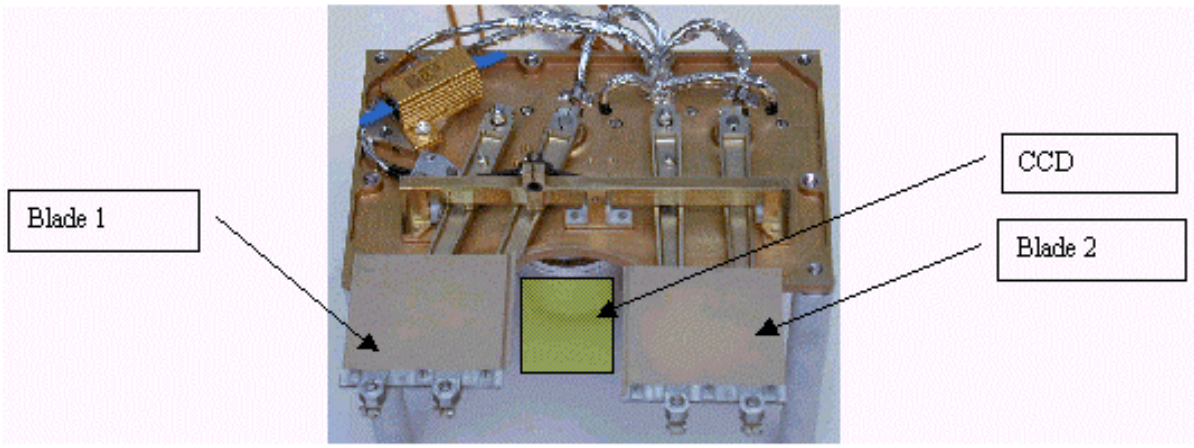

Fig. 14– *The shutter for the WAC and the NAC.*

A customized encoder is associated to each blade to detect its position, and the exposure time. The two actuators are matched in terms of speed thanks to the shutter electronic board: uniform exposure is maintained with no additional speed controller, regardless of position. It is also crucial to maintain the same reference starting point. In addiction another position-sensor is mounted on the shutter, to determine if the first four-bar-mechanism has made his complete travel. Two other mechanisms are located on the shutter: the latch mechanism and the fail-safe mechanism. The first one allows long exposure times without the need of power, blocking the four-bar mechanism in the open position. The fail-safe mechanisms enables, in case of unrecoverable mechanism failure, the frame transfer CCD reading modality: it forces the first blade to cover half CCD while the second blade is blocked in the starting position. The linear speed of the two blades is 1000 mm/s, the distance from the focal plane is about 10mm, the plane of the shutter blade is parallel to the CCD plane, the aperture is parallel to the CCD column. For the WAC the light beam has a cross-section, on the blade plane, of 1.786mm. The travel time over the beam is of 1.795 ms, over the entire clear aperture of the CCD (2048x0.0135+1.795 = 29.443 mm) is 29.44ms. The FoV of 12 deg is covered in 27.64 ms, namely with an angular speed of 1563”/ms (78 pixel/ms).

The blade velocity is measured by means of an optical encoder mounted on the same shaft of each motor, in this way avoiding flexible couplings and minimizing space and mass. The

resolution is 3600 ppr with two channels in quadrature, that leads to a position resolution of about 0.08 mm. In order to satisfy the long-term stability required by the ROSETTA mission, a self-calibration capability was added. By the encoder measurement of the blades motion and the current waveform fed to the motors, it is possible to identify the mechanical parameters of the shutter by means of an ARMAX algorithm. The estimated parameters fed to the inverted dynamics allow change the current profile in order to maintain the velocity constant and so the exposure time uniform over the CCD.

Therefore the advantages of this shutter are the following,

- constant actuation time versus the exposure times. The relative distance between the two moving blades in fact, determines the exposure time
- the exposure time can be changed continuously by changing the delay of actuation of one blade with respect to the other
- uniform exposure of the image. Thank to the two moving blades concept, the exposure time is determined by the slice between the two blades that move across the detector
- exposure times as short as 10 ms can be achieved
- possibility to update in flight the waveform for the each motor.

The shutter electronics

The shutter electronics has the purpose to manage, check and control the shutter mechanism. It is split into two modules: digital and analogue.
The first module store the current waveforms inside two FIFOs, that actuate the blades, by means of a Digital Control Unit that supervise the entire SHE managing the sequences of the shutter actuations. The current waveforms stored into the two FIFOs can be different allowing the activation of the two blades with dedicated waveforms. The Digital Control Unit checks continuously the status of the memories and checks also the functionality of the mechanism during the activation of the blades. This means the SHE can detect 11 different types of probable malfunctions of the entire sub-system and react to them immediately sending the actual status to DPU. The DPU reacts delivering to SHE a new data packet and then SHE autonomously solves the error setting the system in normal operations. The second module is composed by capacitor sets, current drivers supplied by them and other analog parts necessary to control the charge of the capacitors. The sets of capacitors are needed to actuate the blades with a peak power of about 20 watts for the acceleration phase (10ms) and the same amount of power for the deceleration phase(10ms) of each blade. In flight condition, it is possible to adjust the current waveforms stored in the memories by a ground telecommand if some of its parameters (like springs, friction or the performances of the torque motors) are varied, in order to achieve the requested performance of the shutter. Furthermore it is possible to perform an in-flight calibration of the shutter by means of a particular setting of the SHE. There are three different operative modes implemented in the SHE that set the minimum time between consecutive actuations of the shutter. They are fast, nominal and slow. When operating the SHE in fast mode, the minimum time to make consecutive activations of the mechanism is dependent only from the come back time of the blades. DPU sends to the SHE information about the current waveforms necessary to actuate the blades and decides the start of the blades. SHE, after a signal digital conditioning, sends to DPU the blades displacement pulses coming from the two encoders, in order to be stored with the related image.

The front door mechanism

The Front Door Mechanism (FDM) is designed to achieve the double function to protect the optical devices inside the WAC and the NAC, and to perform an in-flight calibration of the telescopes. The door of the mechanism is normally placed over the external baffle of the camera to prevent contamination of the telescopes during the cruise-phase. During the operational one, its

activation makes the door translate and rotate to permit data acquisition. The total number of aperture-closure cycles is foreseen around 5000. The opening motion is performed by keeping the door always parallel to itself, avoiding the direct exposure of the inner surface of the door to the dust environment. The shape of the calibrating side of the cover is designed to obtain a dust-tight closure together with the external baffle. **Fig. 15** shows the EM model of the WAC mechanism (the only difference with the NAC being the shape of the cover, round in case of the NAC). The Front Door Mechanism is provided with a safety device to perform opening of the door in case of failure of the main mechanism.

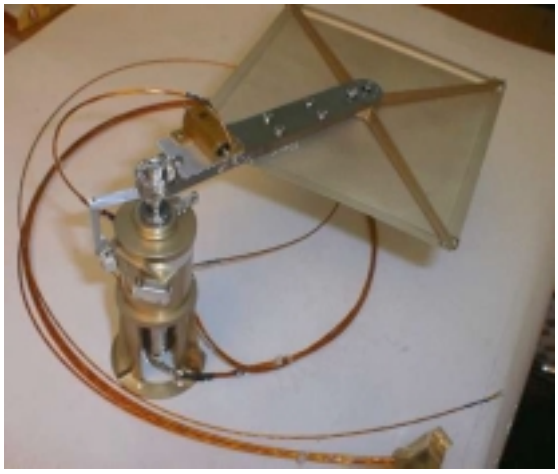

The FDM is mainly composed by the following parts:

- support flange
- cam mechanism
- stepper motor
- bracket
- door.

Fig. 15– *The front door mechanism.*

The mechanism is activated by a gear-head stepper motor with a step angle of 0.3° so that the position of the cover can be known. Two ABB micro switches are employed to detect both opened and closed position. The cam mechanism is composed by an external and an internal cam: the internal cam is moved by the motor, while the external one is fixed to the flange. The coupling of the two cams allows the transformation of the rotary motion into four different phases: unlocking, translation, rototranslation and locking. The time estimated for these phases is 30 s. Due to the peculiar cams design and the reduction gear, the mechanism is irreversible, both in closed and opened position. By reverting the energising of the motor the door is opened or closed.

Fail-safe mechanisms

The Front Door Mechanism is provided with a safety device to perform opening of the door in case of failure of the main mechanism. When the shape memory alloy is actuated, a spring mechanism lifting and rotating constraints the cover in a predefined opened position clearing the FOV of the camera. The rotation is limited to 90°. Two failure cases are foreseen:

a. The door does not start;
b. The door is blocked in an intermediate position.

If, after energising the motor, no signal comes from micro-switch 1 after 90 s (30 s plus 60s) (case a) or if no signal comes from any micro-switch (case b) the safety device will be activated, maintaining permanently the door in opened position.

The OSIRIS CCDs

The NAC and the WAC use identical CCD detectors (back-side illuminated EEV CCD42-40 non-MPP devices). These CCDs feature the desired pixel size and an excellent wide-band quantum efficiency (QE). High dynamic range and sufficiently low power consumption makes them applicable for space operations. In course of improvements, lateral (shielded) anti-blooming overflow protection was introduced to the OSIRIS devices so that weak cometary features can be imaged near bright regions in long duration exposures. The advantage of lateral anti-blooming is

that the quantum efficiency of the detector is not affected. Nevertheless, the full well charge capacity is reduced from 140,000 e^- to about 100,000 e^- per pixel.

The comparatively fast readout keeps the dark charge accumulation low even at room temperatures. With clock dithering applied during exposure, useful images can be obtained with exposure times of up to 40 s at room temperatures. We found the dark charge being significantly more uniform with dithering. The dark current becomes negligible at temperatures below 200 K.

Assume that a V=0 star produces 10^3 ph cm^{-2} s^{-1} A^{-1} at 535 nm. The filter is 600 A wide, its transmission is 80%, the CCD QE is 50%, the reflectivity of the 2 mirrors is 80%, therefore the expected efficiency is as in **Table 6**:

Table 6 – *The WAC expected efficiency for stellar sources*

f(V= -15.0) = $1.0x10^{12}$ counts/s	f(V= 5.0) = $1.0x10^4$
f(V= -10.0) = $1.0x10^{10}$	f(V= 10.0) = $1.0x10^2$
f(V= -5.0) = $1.0x10^8$	f(V= 10.0) = $1.0x10^2$
f(V= 0.0) = $1.0x10^6$	f(V= 12.5) = 10

The 12^{th} mag is therefore the limit in respect to the CCD read out noise.
Regarding the sky background, if it is V=22.0 mag/$arcsec^2$, then given the px size of 20x20 $arcsec^2$, it corresponds to 19 mag/px. Even for superpixel binning 4x4 it becomes of 17.8, totally negligeable. At 3.3 AU, the apparent visual mag of the Sun is 2.5mag dimmer than at 1 AU, namely = -26.7 + 2.5 = -24.2. Suppose that the nucleus is a disk of 1 km^2 area reflecting 5% of the Sun light; at a distance of $1x10^6$ km and at opposition, the apparent mag of the nucleus is -24.2+ 2.5log(5%) + 5log(10^{-6}) = 9.1. At 90° elongation, assuming that only 50% of the surface is visible and neglecting phase effects, the mag is raised to 9.9, still comfortable in respect to the readout noise. Therefore the primary requirement of detection of comet and asteroids in 1s at 10^6 km is satisfied.

The mechanism control board

CISAS has also provided for the WAC and the NAC the Mechanism Controller Board, MCB, that drives the mechanisms (FDM, FWM) and performs housekeeping data acquisition of the two OSIRIS cameras. The MCBs, which are located inside the main electronic box of OSIRIS, consist of two boards, the Control Board and the Drivers Board, mounted on the MCB frame with inward facing components. Interconnecting MTB-1 connectors (ESA SCC 3401/031) were selected for their low profile. Connection to the E-Box interface, (EFI), is made by a KNC 0621310219, 62 pin, connector. Two DB62S connectors, 62 pins, make connections to both the NAC and WAC. The subsystem overall mass is 602 g. The Control Board contains the digital circuits for communication and mechanism control. The analogue housekeeping and position monitor circuits are also mounted on this board. The digital control circuits are implemented by using two Field Programmable Gate Arrays, (FPGA). Data exchange with the DPU module is established using RS-422 line drivers and receivers (HS-26C31/32). Data gathering, packaging, transmission and command decoding are performed within the FPGAs (RH1280). The FPGAs also translate the DPU mechanism commands into motor phase drive programmes that are passed to the motor drivers mounted on the Drivers Board. Full dual redundancy has been employed for the line drivers, digital circuits and the analogue conversion circuits. The two analogue data gathering circuits can read data from single temperature sensors regardless of which circuit is in use. Similarly, either the main or the redundant digital circuits can read the single position monitors from all mechanisms. The Drivers Board, although physically connected to the Control Board, is electrically insulated from it by optical coupling and power supply. The board performs the power translation of the phase signals from the Control Board to the mechanism motors. Each motor has four main phase drivers and four redundant phase drivers. In each of the two cameras there are three motors, giving a total of 48

phase drivers. Either the main or the redundant Control Board digital circuit can program all 48 phases.

Publications

- Da Deppo, V., Naletto, G., Nicolosi, G., Zambolin, P., Pelizzo, M., Barbieri, C., 2001*, Optical Performances of the Wide Angle camera for the Rosetta mission: preliminary results*, SPIE, San Diego Aug. 2001
- Naletto, G., Da Deppo, V., Pelizzo, M. G., Ragazzoni, R., Marchetti, E. 2001*, The optical design of the Wide Angle Camera for the Rosetta Mission*, Journal of the Optical Society of America, 2001
- Debei, S., Fornasier, S., Barbieri, C., Brunello, P., Peron, F., 2001, The Wide Angle Camera of Rosetta mission: design and manufacturing of a baffling system for an innovative optics, SPIE AM115, San Diego Aug. 2000
- Brunello, P.F., Peron, F., Fornasier, S., Barbieri, C., 2000*, Baffling system for the Wide Angle Camera (WAC) of ROSETTA mission*, SPIE, San Diego Aug. 2000
- Doressoundiram, A., Weissman, P.R., Fulchignoni, M., Barucci, M.A., LiBras, A., Colas, F., Lecacheux, J., Birlan, M., Lazzarin, M., Fornasier, S., Dotto, E., Barbieri, C., Sykes, M.V., Larson, S., Hergenrother, C., 1999, *4979 Otawara: flyby target of the Rosetta mission*, Astron&Astrophys 352, 697
- N. Samarasinha, H. Boehnardt, L.Jorda, F.Marzari, B.Mueller, D.Scheeres, 1999, *Rotation Model of Comet 46/P Wirtanen*
- N. Thomas, H.U. Keller, E. Arijs, C. Barbieri, M. Grande, P. Lamy, H. Rickman, R. Rodrigo, K.-P. Wenzel, M.F. A'Hearn, F. Angrilli, M. Bailey, M.A. Barucci, J.-L. Bertaux, K. Briess , J.A. Burns, G. Cremonese, W. Curdt, H. Deceuninck, R. Emery, M. Festou, M. Fulle, W.-H. Ip, L. Jorda, A. Korth, D. Koschny, J.-R. Kramm, E. Kurt, M.L. Lara, A. Llebaria, J.J. Lopez-Moreno, F. Marzari, D. Moreau, C. Muller, C. Murray, G. Naletto, D. Nevejans, R. Ragazzoni, L. Sabau, A. Sanz, J.-P. Sivan, G. Tondello, *OSIRIS - The Optical Spectroscopic, and Infrared Remote Imaging System for the Rosetta orbiter*, Adv. Space Res. 21(11), pp. 1505-1515, 1998.
- Rossi, A., Marzari, F., Farinella, P., 1998, *Orbital evolution around irregular bodies*, Earth, Planets, Space, submitted
- M.A. Barucci, A. Doressoundiram, M. Fulchignoni, M. Florczak, M. Lazzarin, C. Angeli, *Compositional type characterization of Rosetta asteroid candidates*, Planet. Space Sci.,1998, 46, 75
- R.Schulz, C.Arpigny, J.Manfroid, J.A.Stuwe, G.P.Tozzi, K.Rembor, G.Cremonese, S.Paschke, 1998, *Spectral evolution of ROSETTA target comet 46P/Wirtanen*, Astron.&Astrophys., 335, L46
- G.Cremonese, M.Fulle, F.Marzari, V.Vanzani, 1997, *Orbital evolution of meteoroids from short period comets*, Astron. & Astrophys., 324, 770
- M. De Cecco, F. Angrilli, R. Da Forno, S. Debei, 1997, *Uniformity error reduction by adaptative control of an electro-mechanical shutter for space imaging*, in "Developing business from space", 48th International Astronautical Congress, IAF p. 73, Torino 4-10 Ottobre 1997
- Marzari, F., Tomasella, L., Vanzani, V., 1996, *Rosetta Mission: orbital motion around a cometary nucleus*, Lunar and Planetary Science, vol. 27, 823
- Scheeres, D.J., Marzari, F., Tomasella, L., Vanzani, V., 1996, *Rosetta Mission: satellite orbits around a cometary nucleus*, Planetary and Space Science, 46, 649-671
- G. Naletto, E. Marchetti, R. Ragazzoni*, Two-mirror planetary camera with an off-Rowland UV spectrograph for the Rosetta mission*, in Space Telescopes and Instruments II, SPIE Proc. 2807, pp. 238-247, 1996.
- Barucci, A., Lazzarin, M., 1995, *Visible Spectroscopy of the ROSETTA Asteroid Targets: 3840 Mimistrobell and 2530 Shipka*, Icarus 118, 216, 1995
- R. Ragazzoni, G. Naletto, C. Barbieri, G. Tondello, *An optical design for the Rosetta Wide Angle Camera*, in Space Telescopes and Instruments, SPIE Proc. 2478, pp. 257-268, 1995.
- R. Ragazzoni, G. Naletto, M. Turatto, E. Marchetti, *Preliminary optical design for Plures and Rosetta*, in Ultraviolet Technology V, SPIE Proc. 2282 , pp. 162-167, 1994.